GLOBAL JOURNAL OF PURE AND APPLIED SCIENCES VOL. 11, NO. 1, JANUARY 2005: 63 - 71
COPYRIGHT(C) BACHUDO SCIENCE CO. LTD. PRINTED IN NIGERIA. ISSN 1118-0579

SYNTHESIS AND THERMAL CHARACTERIZATION OF POLYPROPYLENE/ ALUMINUM COMPOSITES

J. K. SARAKA, P. GBAHA, A. BOUDENNE, E. GEHIN and Y. CANDAU

(Received 24 March 2004; Revision Accepted 5 August 2004)

ABSTRACT

The present work investigates the heat transfer and specifically, thermal conductivity, diffusivity and specific heat in Aluminium composite materials. The composites were obtained by mixing polypropylene (PP) with oxidized Aluminium (Al) under various volume fractions. Two sizes of filler are used in the sample composite preparation. A nonlinear least-square criterion is used on experimental transfer functions to identify the thermal conductivity and the diffusivity of polypropylene/Aluminium (PP/Al) composites. The thermal parameters of the PP/Al composites having two sizes were determined through identification procedure. Then the density measurements were also carried out in order to deduce the specific heat and thereafter they were compared to values given by differential scanning calorimetry (DSC) measurement. The theoretical results are compared with the experimental ones. Both the Agari and Bruggeman models provide a good estimation for thermal conductivity. Both thermal conductivity and diffusivity show a better heat transport for the composite having large particles, and the heat transfer in this case combine the contribution of phonon and electron transport mode.

KEYWORDS: Thermal properties, polypropylene/Aluminium, material composites.

INTRODUCTION

The use of composites in optoelectronics (*Gaponik et al., 2000*), microelectronics (*Chen et al., 2002*), aeronautics and space transport (*Korab et al., 2002*) is continually increasing. The interest for these materials arises due to the adaptable properties suitable for specific applications. In recent years, there has been increasing interest in the synthesis of organo-inorganic composite materials such as polypyrrole/Palladium (*Cioffi et al., 2000*), polyimide/silver (*Huang et al., 2001*), polypyrrole/Cadmium/Tellurium (*Gaponik et al., 2000*), poly (3,4-ethylenedioxythiophene) PEDOT/V_2O_5 (*Vadivel-Murugan et al., 2001*) and polypyrrole/LiMn2O4 (*Vadivel-Murugan et al., 2001*).

Our area of interest is devoted to the study of physical properties of polymeric materials incorporating metallic particles, and their thermal behavior. Some polymers are considered as thermal insulators due to the low value of their thermal conductivity, whereas metals are good thermal conductors. By mixing these two materials, we can obtain composite with properties, which are intermediate between metallic and polymeric ones. These specific composites are of a great interest because when a metallic filler is above a given concentration, the so-called percolation concentrat ion, electrical properties are close to metals, whereas their mechanical properties are comparable with polymers (Mamunya et al., 2002).

We present here the results of thermophysical study of polypropylene (*PP*) composites filled with oxidized Aluminium (*Al*) under various volume fractions and for two filler sizes.

MATERIALS AND METHODS

Filler distributions

Two oxidized Aluminium filler particles were used having different particle size (*Goodfellow*^{TM}). In order to reach high maximum packing fraction in the composite, it is necessary to use particles with a large distribution size. The granulometric parameters of both fillers were obtained using a LS 230 (Beckman Coulter^{TM}) device, based on a light scattering method. The curves of the particle size distribution are shown in Figure 1. The filler designated $Al_{(A1)}$ is composed of small particles with a mean diameter of 8 μm whereas the filler designated $Al_{(A2)}$ is composed of particles of 44 μm mean diameter. The particle size distribution is contained within narrower limits for $Al_{(A1)}$ than for $Al_{(A2)}$.

J. K. SARAKA, Laboratoire de Froid et Thermique, Institut National Polytechnique de Yamousssoukro, Cote d'Ivoire
P. GBAHA, Laboratoire de Froid et Thermique, Institut National Polytechnique de Yamousssoukro, Cote d'Ivoire
A. BOUDENNE, Centre d'Etude et de Recherche en Thermique, Energetique et Systemes, IUT de Creteil, Universite Paris 12 Val de Marne, 61 Avenue du General de Gaulle, 94010 Creteil Cedex, France
E. GEHIN, Centre d'Etude et de Recherche en Thermique, Energetique et Systemes, IUT de Creteil, Universite Paris 12 Val de Marne, 61 Avenue du General de Gaulle, 94010 Creteil Cedex, France
Y. CANDAU, Centre d'Etude et de Recherche en Thermique, Energetique et Systemes, IUT de Creteil, Universite Paris 12 Val de Marne, 61 Avenue du General de Gaulle, 94010 Creteil Cedex, France

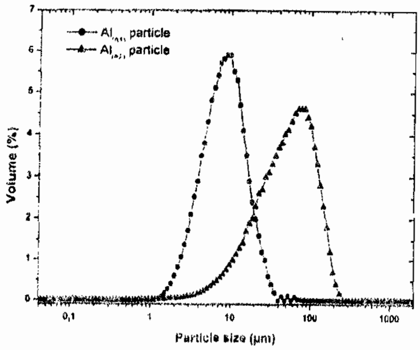

Figure 1. Differential distribution of Aluminium particle size

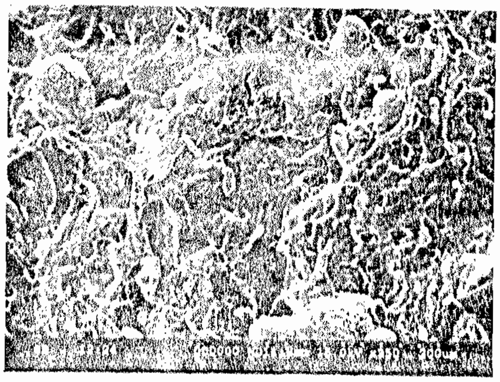

Figure 2. SEM micrograph for 10% of theoretical $Al_{(A2)}$ volume fraction in the PP matrix

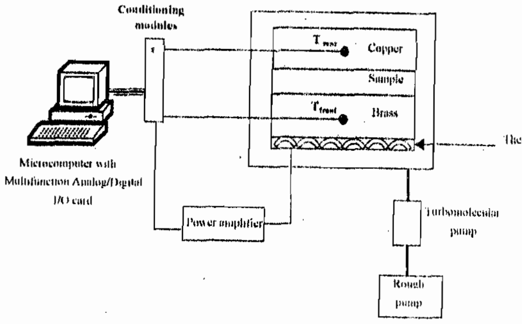

Figure 3. Schematic view of the experimental setup

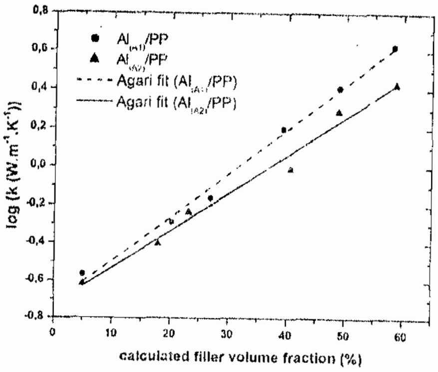

Figure 4. Logarithms for thermal conductivity of $Al_{(A1)}$/PP and $Al_{(A2)}$/PP composites: experimental values and the Agari model

Sample preparation

The composites were prepared by mixing pellets of polypropylene (*PP*) provided by *Finapro(7060)*^{TM} with the Aluminium (*Al*) powders in a 68 cm^3 mixing chamber of a Rheomix mixer (*Haake-Polylab*^{TM}) at 180°C, for 12 minutes and using a mixing speed of 25 rpm. The polymer and the powder were mixed until the stabilization of the torque, which indicates a good filler dispersion in the matrix. Then, composite samples (plates of 10 cm × 10 cm and 3 mm thickness) were obtained by compression molding at 195°C, under a pressure of 200 bars for 5 minutes. The dispersion of the filler in the polymeric matrix is very important in this study because many theoretical prediction models assume homogeneous filler dispersion in the matrix (*Godovsky et al., 1995; Mottram et al., 1991*). Consequently, the overall morphology of composites was studied by SEM observation. The observed surfaces were obtained by breaking the samples at liquid nitrogen temperature. Figure 2 displays the microstructure of a composite sample containing 10% of theoretical volume fraction of $Al_{(A2)}$. Theoretical volume fraction is calculated from the volume of Aluminium powder put in the mixing chamber before the composites realization. It can be clearly seen that the Aluminium particles are randomly dispersed and surrounded by the polymeric matrix. We can also see that the filler particles have different sizes and are not perfectly spherical. The same observations were made for the other filler concentrations.

Thermal conductivity and diffusivity measurement

The experimental setup of thermal conductivity and diffusivity measurement is shown in Figure 3. The sample under study was fixed between the two metallic plates made of brass and copper. A good thermal exchange between the different elements was insured by thermally conductive grease. The front side of the brass plate was heated periodically with a thermoelectric cooling device. The assembled plate was placed in a vacuum chamber connected to a pumping system. The rear side of the copper plate was in contact with air at ambient temperature and a pressure of 10^{-5} mbar. The excitation voltage of the thermoelectric cooling device is the sum of five sinusoidal signals (*Mattei et al., 2000*) The thermocouples (K-type) were placed inside both the front and rear metallic plates. The experimental heat transfer function is calculated at each excitation frequency using (*Söderströn et al., 1989*):

$$\tilde{H} = \frac{FFT(T_{rear}).FFT(T_{front})^{*}}{FFT(T_{front})^{2}} \qquad (1)$$

where, $FFT(T_{front})$ and $FFT(T_{rear})$ are respectively the fast Fourier transform of front and rear temperature, and $FFT(T_{front})^{*}$ is the fast Fourier transform complex conjugate of front temperature. The estimation of both thermal conductivity ($\hat{k}$) and diffusivity ($\hat{a}$) parameters is done simultaneously. The identification procedure consists in finding the set of parameters $\hat{B}$ that minimize the following criterion:

$$S\left(\hat{B}_{k,a}\right) = \sum_{i=1}^{N} \left[\left(\tilde{H}_{real}(f_i) - H_{real}(f_i) \right)^2 + \left(\tilde{H}_{imag}(f_i) - H_{imag}(f_i) \right)^2 \right] \qquad (2)$$

where $\left(\tilde{H}_{real}(f_i)\right)$ and $\left(H_{real}(f_i)\right)$ are respectively the real parts of the experimental and theoretical transfer function, and $\left(\tilde{H}_{imag}(f_i)\right)$ and $\left(H_{imag}(f_i)\right)$ are the imaginary part of the experimental and theoretical transfer function. $\hat{B}$ is the vector of the two estimated parameters ($\hat{k}$ and $\hat{a}$) and N is the number of experimental data. The theoretical transfer function is given by quadrupole theory (*Wang et al., 2002*). The identification of thermal conductivity and diffusivity was achieved using the Levenberg-Marquard method (*Moré, 1977*). The variance-covariance matrix of the estimated thermal property vector $\hat{B}$ can be approximated as:

$$\operatorname{cov}\left(\hat{B}\right) = \sigma^2 \left(J\, J^T\right)^{-1} \qquad (3)$$

where, J represents the Jacobian matrix and J^T the Jacobian transpose. σ represents the standard deviation of the measurements and is estimated by:

$$\sigma^2 = \frac{S}{N-q} \qquad (4)$$

where, N is the number of experimental data and $q = 2$ is the number of identified parameters.
Finally, the approximate statistical confidence bounds of the estimated thermal conductivity and diffusivity values at 95% confidence bounds are respectively: $U(k) = 2\sigma_{\hat{k}}$ and $U(a) = 2\sigma_{\hat{a}}$. We shall use these values as uncertainties for our measurements. So the results obtained can be expressed for respectively the thermal conductivity and the thermal diffusivity respectively as: $k = \hat{k} \pm U(k)$ and $a = \hat{a} \pm U(a)$.

Differential scanning calorimetry (DSC)

The calorimetric measurements were carried out on a Perkin Elmer Pyris 1 series differential calorimeter under a flowing neutral atmosphere. The temperature and heat flow scales were calibrated using high purity indium and tin samples for crystallinity measurements at high temperature, and indium and mercury for specific heat capacity measurements at lower temperature.

DSC measures the heat flow rate $\frac{dH}{dt}$ as a function of temperature. From this measurement, the specific heat capacity c_p may be calculated using this equation:

$$c_p = \frac{\left(\frac{dH}{dt}\right)}{m\ q_H} \qquad (5)$$

where m is the sample mass and q_H is the scanning rate temperature.

This equation may be used directly; nevertheless, mistakes due to the drift of the signal lead to the use of another method. A standard sapphire disc is studied in the same experimental conditions as the sample and the knowledge of the specific heat capacity of the sapphire at all temperatures allows the sample c_p to be calculated.

The following procedure is first applied on the empty pan and lid, next on the sapphire inside the same pan and lid, and finally on the sample inside the same pan and lid: it is held for 5 min at 0°C, then heated from 0°C to 40°C at 10°C/min and held for 5 min at 40°C.

Then the data are shifted in order to superimpose the end of the first isotherms. Indeed, when there is no drift of the signal during the experiment, the heat flows measured during the first and the second isotherms are the same. If not, a slope is subtracted from the signal to superimpose the second isotherms. Then the signal of the empty pan and lid is subtracted from the sample and sapphire signals.

The specific heat capacity of the sample can then be calculated using this equation:

$$c_{p(sample)} = c_{p(sapphire)} \frac{m_{(sapphire)}}{m_{(sample)}} \frac{\frac{dH}{dt}_{(sample)}}{\frac{dH}{dt}_{(sapphire)}} \tag{6}$$

Sample weights were of approximately 14.0 ± 0.1 mg and sapphire weight of 28.42 mg.

Density measurement

The density balance was used in order to know the volume percentage at room temperature of the composite plates studied for the thermal conductivity and diffusivity measurements. Measurements were achieved for square plate samples (45×45×3 mm^3) with a *Mettler-Toledo*^{TM} *AT61* delta range balance.

According to Archimedes' principle, a body immersed in a liquid receives a pressure equal to the displaced liquid. Therefore, by knowing the density of the liquid, it is simple to calculate the volume of the sample and its specific mass. The density which is the inverse of specific volume, may be calculated from equation 8 after the determination of the weight P_a of the sample in the air, and of the weight of the sample P_w in a liquid of d_w density. Distilled water was used as the liquid.

$$d = \frac{P_a}{P_{H_2O}} = \frac{P_a}{\frac{P_a - P_w}{d_w}} = \frac{d_w P_a}{P_a - P_w} \tag{7}$$

The weight concentration of the samples studied by DSC was measured by thermogravimetric analysis (TGA) (Setsys 1200 from Setaram). The samples were heated at 10°C/min beyond the degradation temperature of the polypropylene (600°C). The density values used for the calculation of the composite filler volume fraction are 2.7 $\mathrm{g.cm^{-3}}$ for the Aluminium and 0.91 $\mathrm{g.cm^{-3}}$ for the polypropylene.

Thermal conductivity models

In this section, some thermal conductivity models are presented. Many theoretical and experimental models have been proposed to predict the effective thermal conductivity of composite materials. The Bruggeman model is one of the most effective thermal conductivity prediction model and in addition this model takes into account the filler geometry (*Wong et al., 1999*). This approach is based on the assumption of isolated filler particles by using the following equation [5,8]

$$1 - \phi = \frac{k_c - k_f}{k_m - k_f} \left(\frac{k_m}{k_c} \right)^{\frac{1}{1+x}} \tag{8}$$

where k_c, k_m, k_f are respectively the thermal conductivity of the composite, of the polymer matrix and of the filler. ϕ is the filler volume fraction, and x is the constant which depends on filler geometry: $x = 2$ for spherical particles and $x = 1$ for cylinders.

One other approach for a thermal conductivity prediction model was initiated by Torquato for dispersed spherical or cylinder particles (*Torquato, 1984*). This approach also takes into account the filler geometry and the statistical perturbation around each filler particle. For these bounds, the microstructural parameters was derived using a set of statistical functions (*Boudenne et al., 2003*):

$$\frac{k_c}{k_m} = \frac{1 + \phi\beta - (1-\phi)\zeta\beta^2}{1 - \phi\beta - (1-\phi)\zeta\beta^2} \tag{9}$$

with

$$\beta = \frac{k_f - k_m}{k_f + (d-1)k_m} \tag{10}$$

where d is the constant for the dimension of the system (d = 3 for the sphere particles) and ξ is the microstructural three-point parameter range ($0 < \xi < 1$) for symmetric cell materials with spherical cells of the same size for fully penetrable and impenetrable spheres.

A semi-empirical approach was proposed in order to predict the thermal conductivity of generalized

Table 1. Thermal conductivities and associated uncertainties of composite samples studied

Vol % of $Al_{(A1)}$ calculated from density results	k_1 ($W.m^{-1}.K^{-1}$)	$\frac{U(k_1)}{k_1}$ (%)	Vol % of $Al_{(A2)}$ calculated from density results	k_2 ($W.m^{-1}.K^{-1}$)	$\frac{U(k_2)}{k_2}$ (%)
0.0	0.239	0.38	0.0	0.239	0.38
5.0	0.242	0.74	5.0	0.271	1.18
17.8	0.394	0.81	20.1	0.515	0.66
23.1	0.580	0.34	26.9	0.691	0.80
40.5	0.980	0.44	39.3	1.580	1.08
48.8	1.950	0.91	48.9	2.575	1.24
58.7	2.677	1.49	58.3	4.222	1.37

k_1 is the thermal conductivity of $Al_{(A1)}/PP$ composite
k_2 is the thermal conductivity of $Al_{(A2)}/PP$ composite

Table 2. Values of Agari model coefficients (C_1 and C_2)

Composites	C_1	C_2
$Al_{(A1)}/PP$	0.78 ± 0.08	0.51 ± 0.04
$Al_{(A2)}/PP$	0.78 ± 0.06	0.65 ± 0.03

dispersions (including spherical and irregular particles and fibers) (*Agari et al., 1986*). This approach was based on the generalization of series and parallel conduction models in the composite. The logarithmic equation of Agari and co-workers is given by (*Agari et al., 1993*):

$$\log k_c = \phi C_2 \log k_f + (1-\phi)\log(C_1 k_m) \tag{11}$$

where C_1 and C_2 are experimentally determined constants. C_1 represents the effect of particles on the polymer structure and C_2 represents the ease in the formation of first particle conductive chains.

RESULTS AND DISCUSSION

Thermal conductivity

The identification procedure was applied to the determination of thermal parameters for several samples with increasing Aluminium volume fillers. The thermal conductivity values for the PP/Al composites and their associated relative uncertainties are presented in Table 1 versus Aluminium volume fraction. The obtained relative uncertainties are low (between 0.34% and 1.5%). The values of the filler volume fraction are calculated from the density measurements. A logarithmic plot of these values as a function of the filler volume concentration is presented in Figure 4. We note that the logarithm of the thermal conductivity increases linearly with the filler volume fraction. At a given filler concentration, the composite filled with $Al_{(A2)}$ has a higher thermal conductivity than the one filled with $Al_{(A1)}$. This difference is more significant at higher filler concentrations. The results obtained in this study are not in agreement with previous works, which show that the thermal conductivity is higher for a composite filled with smaller particles (*Lu et al., 1997*). These authors assume that the thermal conductivity does not depend on the size of filler particles. Nevertheless, the probability of forming conductive chains of fillers is higher in the small filler case.

The thermal conductivity of the composite (*PP/Al*) has been evaluated using the Agari model. The conductivity of the PP matrix and of the Aluminium fillers have been fixed respectively to $k_m = 0.239\ W.m^{-1}.K^{-1}$ (experimental value: see Table 2) and $k_f = 237\ W.m^{-1}.K^{-1}$ (value provided by *Goodfellow*^{TM}). We have already noted that the composite thermal conductivity increases when the filler volume is raised. Moreover, the increase in the logarithmic values for the thermal conductivity is linearly proportional to the filler volume fraction in agreement with Agari's model. The Agari curves are shown in Figure 4. The two parameters C_1 and C_2 , which correspond to the curves, were obtained by identification for the two composite types and are presented in Table 2. The C_1 coefficient of the Agari model does not depend on particle size, whereas the filler size affects C_2. The C_2 value is greater for the larger size filler ($Al_{(A2)}$) than for the smaller ($Al_{(A1)}$) one. Accordingly, given the classical interpretation of the C_2 coefficient values, this means that the formation of a thermal conductivity network in the composite should be more likely with large particles. This result is in disagreement with the literature which supposes that effective thermal conductivity of the composite filled with smaller particles is higher than the one filled with the larger particles (*Agrawal et al., 2000*).

In Figure 5, the thermal conductivity values obtained from the experimental study for (PP/Al) composite are

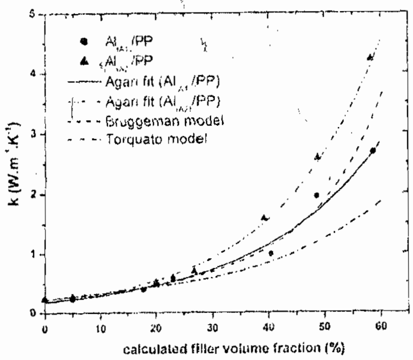

Figure 5. Thermal conductivity for $Al_{(A1)}/PP$ and $Al_{(A2)}/PP$ composites versus calculated volume fraction of filler

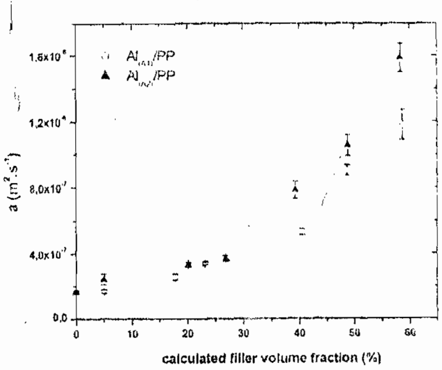

Figure 6. Thermal diffusivity for $Al_{(A1)}/PP$ and $Al_{(A2)}/PP$ composites versus calculated volume fraction of filler

compared with several thermal conductivity models. At low concentration (<15%), we note that all thermal conductivity models give the same values and are in good agreement with the experimental data. For high concentration, both the Bruggeman and Agari models provide a better estimation for thermal conductivity compared to the Torquato model. The Bruggeman model gives a relatively good estimation for the thermal conductivity composite in the case of the smaller filler size. Unfortunately, this last model does not take into account the filler size. The two coefficients (C_1 and C_2) of the Agari model are determined by matching the curve of experimental data and hence, this model represents the data better than other models. Both the Torquato and the Bruggeman models were established from hypotheses on the geometry of the fillers (spherical filler) and their interactions with the matrix. In our case, these hypotheses were not completely verified which explains the divergence between the theoretical model and the measured values of thermal conductivity for the high filler volume fractions. As for Agari's case, the model proposed is semi-empirical, which means that the fit is calculated from experimental data. In these conditions the fit is largely the best one. Nevertheless, it's difficult to give a good physical interpretation of the coefficients fit.

Thermal diffusivity

The thermal diffusivity transport coefficient (*a*) related to the microscopic heat transport of $PP/Al_{(A1)}$ and $PP/Al_{(A2)}$ as a function of the filler concentration is depicted in Figure 6. We observe a nonlinear rise in the composite thermal diffusivity by increasing the filler concentration. This increase in thermal diffusivity is foreseeable because the fillers have a much higher thermal diffusivity than the polymer matrix. Moreover, the thermal diffusivity uncertainty is more significant at higher concentration. It is seen (Fig.6) that composites filled with $Al_{(A2)}$ have higher thermal diffusivity than the ones filled with $Al_{(A1)}$ at the same concentration. For a given concentration, the filler size affects the heat propagation in the composite. As for the case of thermal conductivity, previous results reported by many authors show that the thermal diffusivity is bigger for the smaller fillers than for the larger ones (*Krupa et al., 2001; Lu et al.,1997; Agrawal et al., 2000*). The discrepancies observed between our results and those in the literature will be discussed further in the fifth section of this paper. On one hand and contrary to thermal conductivity, there isn't any theoretical models that predict the thermal diffusivity behavior of composite materials. On the other hand, the thermal diffusivity values can be calculated using the equation 12 knowing c_p , k and d values.

Specific heat capacity

Once thermal conductivity, diffusivities and densities are measured, the specific heat is calculated using the following equation:

$$c_p = \frac{k}{d\ a} \tag{12}$$

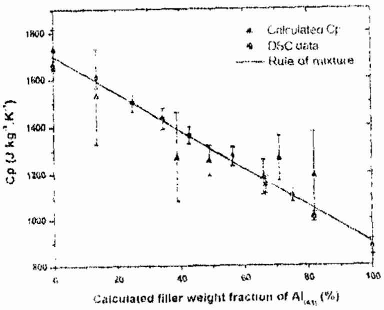

Figure 7. Specific heat for $Al_{(A1)}/PP$ composites versus calculated weight fraction for the computed c_p values and TGA measured weight fraction for DSC data

In order to check the validity of our measurement technique, the specific heat of several samples were measured with another measurement technique (DSC). In Figure 7, the specific heat values obtained from DSC measurements and those calculated from equation 12 are compared for the $Al_{(A1)}/PP$ composite material. The DSC data were obtained for samples of little size. The filler weight fractions of these composites were determined by TGA. The filler weight fractions of calculated c_p were obtained using the values of density measurement. We note a good agreement between the values obtained by the two methods for the low and medium weight fractions. However, for the high weight fractions, the estimated values for specific heat are greater than the ones given by DSC and exhibit also large uncertainty bounds. On the other hand, the rule of mixture can predict correctly the specific heat of the PP/Al composite for all weight filler fraction. Finally, as expected, a linear dependence of the specific heat upon the weight fraction is observed.

DISCUSSION

The C_1 values obtained from the Agari model for the composites having two sizes are not equal to one. According to Agari, this means that the presence of fillers modifies the polymeric matrix. The DSC measurements of the crystallinity percentage have shown that it was not seriously modified by the presence of fillers. The presence of fillers may also have affected the size of the crystals. The fact that the C_1 values are the same for the two filler types is in agreement with the fact that the crystallinity percentages of the composites are not greatly affected by particle size. Otherwise, the crystallinity percentages of the polymeric matrix being the same as that of the composite, it seems that the fillers do not act as nucleating agents. So, the value of C_1 represents here the effect of the fillers on the crystalline phase organization and probably on the polymer crystal size, and not on a change of the crystallinity percentage. Values of C_1 lower than one can be observed even if the crystallinity percentage is not modified by the presence of fillers. This result is in agreement with results reported by Agari et al. (*Agari et al., 1991*) who noted that the C_1 value should depend not only upon the crystallinity nature but also upon crystal size.

Since the thermal conductivity and diffusivity values are higher for the $PP/Al_{(A2)}$ composite, the corresponding C_2 coefficient is also higher. According to Agari, the C_2 coefficient is linked to the probability of easy formation of conductive chains (*Boudene al., 2003; Agari et al., 1987*). Generally in the case of smaller fillers, there is a higher probability of forming conductive chains, so the higher value of C_2 coefficient is observed for the smaller fillers. This result is valid for both conductive and insulating fillers (*Krupa et al., 2001; Agari et al., 1987*).

In our case, the results are different. The C_2 coefficient is greater for the bigger size of the particles. As we mentioned earlier, we have used slightly oxidized Aluminium particles for the preparation of our composites. Electrical conductivity measurements were done and have confirmed that the electric conductivity does not vary with filler concentration and size, but these results are beyond the scope of this paper. Consequently, the composites prepared are electrical insulators even for the higher concentration used. This shows that there is no electron transporting mode in the composite. The heat transport mode in these *PP/Al* composites is not due to electron transport along *Al* chains. But rather the principal heat transport mode in this case is due to the phonons utilizing the free paths. This is explained by the presence of oxide on the surface of *Al* particles. Nevertheless, the results obtained showed significant differences between the thermal conductivity and diffusivity of the two composites ($PP/Al_{(A1)}$ and $PP/Al_{(A2)}$). In our case, the probable explanation is that the large filler particles have a higher proportion of Aluminium than the smaller ones due to the oxide layer which covers the particles. This gives a higher heat transport ability to the $PP/Al_{(A2)}$ composite.

The thermal conductivity value used for the computation of the Agari model coefficients is the one given for pure heavy Aluminium. The effective thermal conductivity of the fillers used in this study is probably lower than this value, and depends also on the mean size of the particles: lower for the small particles ($Al_{(A1)}$) than for the large ones ($Al_{(A2)}$).

Besides, in the case of large particles, the heat transfer may combine the contribution of phonon and electron transport mode. It is likely that the contribution of the electron transport plays a minor role: localized inside the particle and stopped at the oxide layer surrounding the particle. This layer prevents the continuity of the electronic transport mode: the heat propagation between *Al* particles and between *Al* particle and *PP* matrix is restricted to the phonons mean free paths. Finally, we can also mention that this phonon mean path is shorter in smaller particles than in the bigger particles. This also may contribute to lower thermal properties in the case of composites made with the smaller filler size.

CONCLUSION

The thermal conductivity and diffusivity measurements of polypropylene incorporating Aluminium were analyzed and discussed. The density of composite sample plates was measured using a density balance. The weight concentration of DSC samples was determined by thermogravimetric analysis (TGA). The polymeric matrix cristallinity and the specific heat capacity of the samples were achieved with DSC measurements and compared to the one obtained by calculated method. Two sizes of filler were used in the sample composite realization. The thermal conductivity of the composites was compared to theoretical models. Both Agari's and Bruggeman's models provide a better thermal conductivity estimation than the Torquato model. The C_1 coefficient of Agari's model did not equal one although the crystallinity percentage does not change as a function of filler quantity in the matrix. This was explained by the evolution of the polymer crystal size and phase. On the other hand, a higher heat transport ability was observed for the greater particles than for the smaller ones. This result is different from those found in the literature (*Krupa et al., 2001; Agari et al., 1987; Agrawal et al., 2000*), and was explained by the partial oxidation of Aluminium.

REFERENCES

Agari, Y., Ueda, A., Nagai, S., 1993. Thermal conductivity of a polymer composite. J. Appl. Polym. Sci., 49: 1625-1634.

Agari, Y., Ueda, A., Nagai, S., 1991. Thermal conductivity of a polyethylene filled with disoriented short-cut carbon fibers. J. Appl. Polym. Sci., 43: 1117-1124.

Agari, Y., Tanaka, M., Nagai, S., 1987. Thermal conductivity of a polymer composite filled with mixtures of particles. J. Appl. Polym. Sci., 34: 1429-1437.

Agari, Y., Uno, T., 1986. Estimation on thermal conductivities of filled polymers. J. Appl. Polym. Sci., 32: 5705-5712.

Agrawal, R., Saxena, N. S., Mathew, G., Thomas, S., Sharma, K. B., 2000. Effective thermal conductivity of three-phase styrene butadiene composites. J. Appl. Polym. Sci., 76: 1799-1803.

Boudenne, A., Khaldi, S., 2003. Temperature and liquid crystal concentration effect on thermal conductivity of poly(styrene) dispersed 5CB liquid crystal. J. Appl. Polym. Sci., 89: 481-486.

Chen, Y. M., Ting, J. M., 2002. Ultra high thermal conductivity polymer composites. Carbon, 40: 359-362.

Cioffi, N., Torsi, L., Sabbatini, L., Zambonin, P. G. and Zacheo, T. B., 2000. Electro synthesis and characterization of nanostructured Palladium-poly-pyrrole composites. J. Electroanal. Chem., 488 (1): 42

Gaponik, N. P., Talapin, D.V., Rogach, A.L. and Eychmuller, A., 2000. Electrochemical Synthesis of CdTe nanocrystal/polypyrrole Composite for Optoelectronic Applications. J. Mater. Chem., 10 (9): 2163.

Godovsky, Y. K., Privalko, V. P., 1995. Thermal and electrical conductivity of polymer materials, Springer-Verlag: Berlin, pp 1-30.

Huang, J. C., Qian, X. F., Yin, J., Kang-Zhu, Z., Hong-Jie, Xu, 2001. Preparation of Soluble polyimide-Silver nanocomposites by a Convenient ultraviolet Irradiation technique. Mater Chem. Phys., 69 (1-3): 204.

Korab, J., Stefanik, P., Kavecky, S., Sebo, P., Korb, G., Part A 2002. Thermal conductivity of unidirectional copper matrix carbon fibre composites. Composites, 33 : 577-581.

Krupa, I., Chodak, I., 2001. Physical properties of thermoplastic/graphite composites. European Polymer Journal, 37: 2159-2168.

Lu, X., Xu, G., 1997. Thermally conductive polymer composites for electronic packaging. J. Appl. Polym. Sci., 65: 2733-2738.

Mamunya, Ye. P., Davydenko, V. V., Pissis, P., Lebedev, E. V., 2002. Electrical and thermal conductivity of polymers filled with metal powders. European Polymer Journal, 38: 1887-1897.

Mattéi, S., Tang-Kwor, E., 2000. A new periodic technique for thermal conductivity measurement. High temperature - High pressures, 32: 3-8.

Moré, J. J., 1977. The Levenberg-Marquardt Algorithm: Implementation and Theory, Numerical Analysis, ed. G. A. Watson, Lecture Notes in Mathematics 630, Springer Verlag, pp 105-116.

Mottram, J. T., Taylor, R., 1991. International Encyclopedia of composite, vol 5, New York, pp 476-496.

Söderströn, T., Stoica, P., 1989. System Identification, Prentice Hall (UK) Ltd.

Torquato, S., 1984. Bulk properties of two-phase disorder media, I. cluster expansion for the effective dielectric constant of dispersions of penetrable spheres. J. Chem.. Phys., 81(1): 5079-5088.

Vadivel-Murugan, A., Kale, B. B., Kwon, C. W., Campet, G. And Vijayamohanan, K., 2001. Synthesis and characterization of a new organic-inorganic poly(3,4-ethylenedioxythiophene) PEDOT/V_2O_5 nanocomposite by intercalation. J. Mater. Chem., 11(10): 2470.

Vadivel-Murugan, A., Sonwane, R. S. and Kale, B. B., 2001. Synthesis and characterization of high specific capacity of PPY/$LiMn_2O_4$ nanocomposites as positive electrode material for 4V Lithium secondary batteries. Trans. S. AEST, 56(1-2): 49.

Wang, H., Degiovanni, A., Moyne, C., 2002. Periodic thermal contact: a quadrupole model an experiment. Int. J. Therm. Sci., 41: 125-135

Wong, C. P., Boullampally, Raja S., 1999. Thermal conductivity, Elastic modulus, and Coefficient of thermal expansion of polymer composites filled with ceramic particles for electronic packaging. J. Appl. Polym. Sci., 74 : 3396-3403.